Composite core-and-skirt collagen hydrogels with differential degradation for corneal therapeutic applications

Mehrdad Rafat, Maria Xeroudaki, Marina Koulikovska, Peter Sherrell, Fredrik Groth, Per Fagerholm and Neil Lagali

Original Publication:

Mehrdad Rafat, Maria Xeroudaki, Marina Koulikovska, Peter Sherrell, Fredrik Groth, Per Fagerholm and Neil Lagali, Composite core-and-skirt collagen hydrogels with differential degradation for corneal therapeutic applications, 2016, Biomaterials, (83), 142-155.
http://dx.doi.org/10.1016/j.biomaterials.2016.01.004

Composite core-and-skirt collagen hydrogels with differential degradation for corneal therapeutic applications

Mehrdad Rafat[1,2,¥], Maria Xeroudaki[3,¥], Marina Koulikovska[3], Peter Sherrell[1], Fredrik Groth[3], Per Fagerholm[3], and Neil Lagali[3]*

[1]Department of Biomedical Engineering, Linköping University, Linköping, 581 83 Sweden
[2]LinkoCare Life Sciences AB, Linköping, Sweden
[3]Department of Ophthalmology, Institute for Clinical and Experimental Medicine, Linköping University, 581 83 Linköping, Sweden

[¥] denotes equal contributions

*Corresponding author
Neil Lagali, PhD
Department of Ophthalmology
Institute for Clinical and Experimental Medicine
Faculty of Health Sciences
Linköping University
58183 Linköping, Sweden
Tel. +46101034658
Fax +46101033065
Email neil.lagali@liu.se

Abstract

Scarcity of donor tissue to treat corneal blindness and the need to deliver stem cells or pharmacologic agents to ensure corneal graft survival are major challenges. Here, new composite collagen-based hydrogels are developed as implants to restore corneal transparency while serving as a possible reservoir for cells and drugs. The composite hydrogels have a centrally transparent core and embedded peripheral skirt of adjustable transparency and degradability, with the skirt exhibiting faster degradation *in vitro*. Both core and skirt supported human epithelial cell populations *in vitro* and the skirt merged homogeneously with the core material to smoothly distribute a mechanical load *in vitro*. After *in vivo* transplantation in rabbit corneas over three months, composites maintained overall corneal shape and integrity, while skirt degradation could be tracked *in vivo* and non-invasively due to partial opacity. Skirt degradation was associated with partial collagen breakdown, thinning, and migration of host stromal cells and macrophages, while the central core maintained integrity and transparency as host cells migrated and nerves regenerated. **Impact:** This study indicates the feasibility of a collagen-based composite hydrogel to maintain corneal stability and transparency while providing a degradable peripheral reservoir for cell or substance release.

Key words: cornea, porcine collagen, composite, degradation, keratoplasty, femtosecond laser

1 Introduction

Millions worldwide suffer from corneal blindness, a leading cause of visual impairment [1]. Transplantation with human cadaveric tissue is presently the only treatment option in most cases, but severe tissue shortage has led to an urgent need to develop bioengineered alternatives to donor corneal tissue [2-12]. Natural collagen-derived corneal scaffolds are the most mature of these [13-19], and we recently reported results from collagen-based scaffolds four years after implantation into diseased human corneas [13]. These cell-free scaffolds replaced the extracellular matrix, allowing host cells and nerves to eventually grow over and around the scaffold [13].

In blinding corneal conditions, however, such as limbal epithelial stem cell deficiency (LSCD) [20], burn-induced wounds [21] or infection leading to inflammation and neovascularization [22], use of a stromal scaffold alone (human or tissue-engineered) is insufficient – the underlying stem cell deficiency, inflammation and/or neovascularization must also be addressed to avoid eventual graft failure. For patients with LSCD, transplantation of limbal grafts [23] or ex vivo expanded limbal epithelial stem cells [24] is first required. After limbal restoration, central transplantation (keratoplasty) follows to treat scarring in the visual axis. When corneal scarring is complicated with corneal neovascularization and/or severe infections such as herpes simplex keratitis (HSK), anti-inflammatory, anti-angiogenic, antimicrobial or antiviral agents are administered in conjunction with the standard corticosteroid treatment following (or prior to) the high-risk keratoplasties [25]. These therapeutic regimens are most commonly administered topically with the main challenge of low drug penetration through the corneal epithelium. Limited diffusion across the cornea and the increased washing through the tear drainage result in a low bioavailability of 1-7% for most approved drugs [26]. New administration routes, and ideally a controlled-release drug delivery through biodegradable polymeric implants [27], would lead to increased success rates of corneal transplantation in these severe inflamed corneas.

In these high-risk applications, biomaterials are required not only as transparent and robust scaffolds to replace diseased corneal tissue, but also to deliver therapeutics or stem cells into the cornea. These requirements could be opposing – release of cells or substances requires a degree of bio-degradation, however, this could compromise optical transparency and corneal

integrity. Also, requirements of transparency and non-toxicity of biomaterials may complicate the ability to encapsulate, deliver and monitor cells and therapeutic substance release *in vivo*.

Here we introduce new composite tissue-engineered collagen-based constructs to address these requirements. The composites consist of a natural collagen-based core-and-skirt design that functions as a corneal stromal substitute (core) and a biodegradable reservoir for therapeutic drugs and cells (skirt). The central core is a transparent and stable cross-linked collagen hydrogel called the bioengineered porcine construct (BPC) which we have recently reported [14], while the skirt is composed of mechanically-compressed collagen embedded within the BPC scaffold by in situ copolymerization. Physical properties of the skirt (thickness, porosity, mechanical properties) can be tuned for optimal degradation and transparency while the core remains stable over a longer period as a regenerative scaffold. A key feature is tunable transparency to facilitate non-invasive, in vivo tracking of skirt degradation (and thereby cell/substance release) by standard clinical imaging methods.

The aim of the present study was to investigate the properties of the new composite collagen hydrogels in terms of structure, transparency, and degradability, and to determine its degree of biocompatibility, stability, degradation potential, and mechanism of degradation *in vivo* in a model of intra-stromal implantation in rabbits. Composite hydrogels were evaluated with different skirt thicknesses (thin and thick mesh versions) merged within different core materials (standard-crosslinked BPC and hybrid-crosslinked HBPC hydrogels), to investigate their biocompatibility and biodegradation properties. This provides proof of feasibility for future studies investigating the composites after loading with specific therapeutic agents.

2 Materials and methods

2.1 Fabrication of corneal implants

We previously reported the fabrication process for collagen-based corneal implants [14,28]. 1-[3-(Dimethylamino)propyl]-3-ethylcarbodiimide methiodide - (EDCM) and N-hydroxysuccinimide (NHS), Poly(ethylene glycol) diacrylate (PEGDA, M_n =575), Ammonium persulphate (APS) and N,N,N,N- tetramethylethylenediamine (TEMED) were purchased from Sigma-Aldrich (St. Louis, USA). 2- methacryloyloxyethylphosphorylcholine (MPC) was obtained from Biocompatibles (UK). Porcine Collagen (type-I atelo-collagen) was purchased from

Nippon Ham Meat Packers (Tokyo, Japan) and SE Eng Co. (Seoul, South Korea). In this study, increased collagen content within the implant core (18% collagen) was achieved by a controlled vacuum evaporation of a dilute solution (5%) of collagen at room temperature. The 18% solution was then crosslinked using either the water-soluble cross-linking agents EDCM and NHS (BPC core) or a hybrid system comprised of PEGDA, APS, TEMED, MPC, EDCM, and NHS (HBPC core). Crosslinkers were added to the collagen solution, mixed thoroughly and molded between glass plates to make a homogeneous hydrogel scaffold. A 150 μm thick spacer and a clamping system were used for compression molding of the 150μm thick implants. Samples were cured at room temperature and then at 37°C, in 100% humidity chambers. De-molding was achieved by immersion in phosphate buffered saline (PBS) for 1 hour. Samples were subsequently washed three times with PBS solution (1× PBS, containing 1% v/v chloroform) at room temperature to extract reaction byproducts, and to sanitize the samples.

For the composite core-and-skirt design, 1% and 2% solutions of porcine collagen (Nippon Ham) were made and then mixed with 1 x Dulbecco's Modified Eagle Medium (DMEM) at 9:1 ratio. After adjusting the pH to neutral pH and incubation at 37°C, the solution was partially compressed in between two plastic meshes (to form the collagen for the skirt into a nanomesh) and glass plates to partially remove the fluids. Two thicknesses of skirt were fabricated. A collagen concentration of 1% (2%) for the skirt and 50μm (100μm) spacing between the plastic meshes was used to form the thin (thick) mesh. 2mm dia. circular buttons were then cut and removed from the partially compressed gel, to leave skirt-free regions (holes) that would later become occupied by the core material. Thick or thin skirt were then set within the core material (an 18% collagen-crosslinker mixture) and sandwiched between two glass plates with 150 μm spacers. Compression molding allowed the collagen-crosslinker mixture to penetrate into the partially compressed nanomesh forming a single merged mesh-hydrogel composite. The composite was cured at room temperature overnight followed by 6 hrs at 37°C, then demolded and washed in PBS. By this fabrication method, core and skirt regions are interconnected both physically through penetration of core hydrogel into the voids of the skirt nanomesh, and chemically via covalent bonds (chemical cross-links) between collagen fibrils in the core and skirt. Skirt transparency depended on collagen concentration, with the 2% solution resulting in more opacity than 1%. Implants were fabricated as standard

BPC core and skirt composed of thin mesh (MBPC thin) or thick mesh (MBPC thick), or as hybrid-crosslinked core without skirt (HBPC) or with skirt composed of thick mesh (MHBPC thick). As a negative control for cell culture and mechanical tests, polypropylene mesh (BD Biosciences, San Jose, USA) was used to form a fully synthetic skirt, which was subsequently embedded in a BPC core, following the above procedure. A schematic overview of the fabrication process of the composite core-and-skirt hydrogels is given in Fig. 1.

2.2 Light transmission and scatter measurements

Light transmission and scatter were measured at room temperature, with white light (quartz-halogen lamp source) and narrow spectral regions (centered at 450, 550, and 650 nm) using a custom-built optical instrument [29]. 150 µm-thick samples were hydrated in PBS before and during measurements.

2.3 Mechanical properties measurements

The impact of skirt incorporation into core hydrogel materials on mechanical properties was evaluated using an Instron Series IX Automated Materials Testing System (Model 3343, Instron, Canton, MA) equipped with a load cell of 50N capacity and pneumatic metal grips at a crosshead speed of 5 mm/min. Collagen solutions were dispensed and cured in dumbbell – shaped Teflon molds, with ends containing collagen mesh and center remaining mesh-free. A synthetic skirt made from polypropylene (PP) mesh was also incorporated into the ends of some samples for comparison with the collagen-based skirt and to investigate the impact of materials match/mismatch on mechanical behavior of the core-skirt composites. PBS-equilibrated dumbbell specimens were attached to the grips with a pneumatic pressure of 40 psi and immersed in a temperature-controlled container (BioPuls bath) filled with PBS at 37oC during the test.

2.4 Collagenase degradation

To evaluate *in vitro* degradation rate of biomaterials, collagenase Type I (from Clostridium histolyticum) was used as in a previously reported protocol [14]. Briefly, 80 mg samples (150 µm thick) from each biomaterial group were incubated in collagenase-buffer solution. The hydrogels were weighed at different time points after the surface water was gently blotted

away (0, 1, 2, 3, 6, 8, 10, 14, 16, 18 hours). The percent residual mass of hydrogels was calculated according to the ratio of the weight at each time point to the initial hydrogel weight at time zero.

2.5 Evaluation of human corneal epithelial cells growth on bioengineered hydrogel scaffolds.

Immortalized human corneal epithelial cells (HCECs) (American Type Culture Collection, ATCC, Manassas, USA) were used to evaluate cell biocompatibility of the hydrogels. HCECs were seeded in wells within a 96-well cell culture plate without hydrogel (control), on top of 150 mm^2 pieces of collagen composite hydrogels, or PP skirt and collagen-core hydrogels and then supplemented with a serum-free medium optimized for the culture of human corneal epithelial cells (EpiGRO™ Human Ocular Epithelia Complete Media Kit, Millipore, Billerica, MA, USA). Once the control wells became confluent, after approximately 3 days of culture, all wells were stained with the LIVE/DEAD® Viability/Cytotoxicity assay (Invitrogen). Stained cells were photographed with a Zeiss inverted fluorescent microscope using the Zen software (Zeiss LSM700) under a 10x magnification on day 5 post-seeding. Green and red fluorescence corresponded to live and dead cells, respectively.

2.6 Animals and Femtosecond laser-assisted intrastromal keratoplasty (FLISK)

With approval by the Linköping Animal Research Ethics Committee (Application no. 108-12) and following the Association for Research in Vision and Ophthalmology (ARVO) guidelines for the Use of Animals in Ophthalmic and Vision Research, 25 male New Zealand white albino rabbits weighing 3- 3.5 kg were operated. Surgery was performed under general anesthesia with intramuscular injection of 25 mg/kg ketamine (Ketalar 50mg/ml; Parke-Davis, Taby, Sweden) and 5mg/kg xylazine (Rompun 20mg/ml; Bayer, Gothenburg, Sweden). Local anesthetic drops were also used (tetracaine hydrochloride eye drops 1%, Chauvin Pharmaceuticals Ltd., Surrey, UK). The right eye underwent intra-stromal corneal transplantation in all 25 rabbits while left eyes served as untouched negative controls. Operations were performed according to the technique of femtosecond laser-assisted intra-stromal keratoplasty (FLISK), reported previously [14]. An Intralase iFS 150kHz femtosecond laser (Abbott Medical Optics, Solna, Sweden) was used to cut corneal buttons of purely stromal tissue (not including any part of the epithelium or endothelium). The precise

dimensions and location of the buttons to be removed were pre-programmed via the laser's user interface and were identical for all rabbits. For the current study, 3mm diameter buttons of 150µm thick native tissue were removed from a mid-stromal depth (125µm depth from the corneal surface to the anterior surface of the excised button). In all groups, femtosecond laser-cut buttons were manually excised using surgical forceps (through an arc-shaped opening to the corneal surface limited to 70° of the circumference [14], leaving an empty stromal pocket. Immediately prior to implantation of the biomaterials, a 3mm diameter tissue trephine was used to cut circular buttons from 150µm thick flat sheets of the various biomaterials. It was intended that manual trephination would create buttons with a 2 mm central clear core and a 0.5 mm width peripheral translucent skirt. In many cases, however, manual centering was inexact and resulted in crescent-shaped skirt regions that nevertheless contained clearly visible core and skirt regions (due to difference in core and skirt transparency) and were deemed viable for *in vivo* implantation and tracking. Rabbits were divided into 5 groups of 5 rabbits each. In the first (positive control) group, native corneal tissue was cut intra-stromally with a femtosecond laser, excised and thereafter manually inserted again in its former position into the empty stromal pocket using anatomical forceps (autograft transplantation). In the remaining four groups, the FLISK method was identical except that the excised corneal tissue was replaced by one of four different bioengineered implants.

No postsurgical sutures were used because the intra-stromal location and small access cut were sufficient to ensure implants remained in place within the host stromal pocket. After surgery and for the first postoperative day, all operated eyes received antibiotic eye ointment (Fucithalmic 1%, Leo Pharmaceuticals, Denmark) three times daily. The use of steroids (Opnol eye drops 1 mg/mL, CCS Healthcare AB, Borlänge) was minimal and restricted to severely inflamed eyes following operation.

2.7 Postoperative clinical evaluation

Immediately after operation, all operated corneas were photographed with a high-magnification digital camera (Nikon D90 camera, Nikon Canada Inc., Toronto, Canada). Evaluation of intra-stromal location of implants and corneal thickness measurement was performed by Anterior Segment Optical Coherence Tomography (AS-OCT; Visante OCT, Carl Zeiss AB, Stockholm, Sweden) in high resolution mode (average of three thickness

measurements per cornea). The first postoperative week all animals were visually inspected daily for clinical signs of inflammation, and antibiotics and/or steroids were administered as needed. Detailed *in vivo* examinations under general anesthesia were performed at 1 and 3 months following operation. High-magnification digital photography was used to visualize core and skirt, and signs of inflammation, neovascularization and degree of optical transparency. High resolution AS-OCT images were obtained from the same horizontal central cross-section of the operated corneas to measure corneal thickness, evaluate corneal transparency and localize the skirt longitudinally. Laser-scanning in vivo confocal microscopy (IVCM) (Heidelberg Retinal Tomograph 3 with Rostock Corneal Module, Heidelberg Engineering, Heidelberg, Germany) was performed in a manner described in detail elsewhere [30,31] and was used to assess corneal morphology including cell and nerve population in and around the implanted regions. Animals were euthanized by 100mg/kg intravenous sodium pentobarbital (Pentobarbitalnatrium vet APL 60mg/mL, Kungens Kurva, Sweden) at 3 months following operation. Following sacrifice, the central implanted regions were excised and fixed in 4% paraformaldehyde fixative in 0.1M PBS for ex-vivo analysis. Additionally, eight untouched left corneas were excised and served as negative controls.

2.8 Histopathological evaluation

Fixed corneas were imbedded in paraffin and sectioned to 4μm-thickness and hematoxylin and eosin (H&E) staining was performed. For immunohistochemical analysis, sections from paraffin-embedded tissues were deparaffinized, trypsinized and endogenous peroxidase was blocked. Sections were incubated with the following primary antibodies for 30 minutes: mouse monoclonal anti-alpha smooth muscle actin, α-SMA (dilution 1:25, ab 7817, Abcam, Cambridge, United Kingdom), mouse monoclonal anti-type III collagen (dilution 1:100, Acris AF 5810, Germany), mouse monoclonal anti-leukocyte common antigen CD45 (dilution 1:400, Acris AM02304PU-S, Germany). After antibody application and incubation in envision HRP, DAB liquid chromogen was applied to all samples and sections were counterstained with hematoxylin. Samples were dehydrated, cleared in xylene and coverslipped with Mountex mounting medium (Histolab Products AB, Gothenburg, Sweden). In all cases, control samples were used and omission of the primary antibody eliminated specific staining. Light microscopy was performed with an Axiophot Photomicroscope (Zeiss, West Germany) under 10x and 20x magnification.

2.9 Scanning and Transmission Electron Microscopy

Scanning electron microscopy (SEM) was performed using a ZEISS (LEO 1550 Gemini) field emission microscope. The collagen mesh samples were prepared via immersion in liquid nitrogen for 60s followed by lyophilization for 24hours. Samples were sputtered with a 2nm gold coating prior to mounting for SEM. Samples were examined using an accelerating voltage of 3 KeV and a working distance of 3 - 5.5 mm.

For Transmission Electron Microscopy (TEM), fixed samples were imbedded in resin (Epon 812; TAAB, Reading, England). 4µm thick sections were made and stained with toluidine blue dye for light microscopy in order to specify the area of interest. Ultrathin sections of 60 nm were cut from the polymerized block and these sections were collected on 200 mesh copper grids. Finally, the ultrathin sections were stained with uranyl and lead citrate and imaged with a transmission electron microscope (EM JEM 1230, JEOL Ltd., Tokyo, Japan). TEM images were utilized for the quantification of collagen fibril diameter by Image J (Image J software, developed by Wayne Rasband, National Institutes of Health, Bethesda, MD; available at http://rsb.info.nih.gov/ij/index.html). Images depicting different regions were used for collagen fibril diameter measurements in the native corneal stroma, central core and peripheral skirt region (3 images for each). For core and skirt parts, TEM pictures prior to implantation were analyzed. From each image, the diameter of 30 different collagen fibrils was measured.

2.10 Statistical analysis

Thickness of implanted materials measured by OCT was compared using one-way analysis of variance (ANOVA). Change in corneal thickness in the same eyes relative to immediately postoperative and to the final examination was analyzed by the paired t-test. Subbasal nerve density across groups at 3 months postoperatively was compared using one-way ANOVA. Collagen fibril diameter measurements were compared Kruskal-Wallis one-way ANOVA on ranks with Dunn's method to isolate pairwise differences. For all statistical tests, two-tailed significance below 0.05 was considered significant, and all tests were performed with Sigma Stat 3.5 software (Systat Software Inc., Chicago, IL, USA).

3 Results

3.1 Optical, chemical, mechanical and structural characterization of biomaterials

Control of skirt transparency was achieved by varying collagen concentration 1 - 2% and skirt thickness from 50-100 µm (Fig. 2A,B). Light transmission and scatter (Fig. 2C,D) indicated core materials (BPC, HBPC) had similar white light transmission to the native rabbit cornea, while transmission was controllably reduced in the skirt region of the composite hydrogel (MBPC) compared to the core-only material (BPC). Reduced transmission and increased scatter were due to additional compressed collagen fibers in the skirt, which was used to facilitate *in vivo* tracking of implant degradation. HBPC and BPC cores had similar transparency and scatter. Scatter of core materials was elevated (4-5% scatter) relative to the native rabbit cornea (1-2%), while skirt opacity in composites further enhanced scatter (7%).

By *in vitro* collagenase assay, composite hydrogels were less resistant toward collagenase degradation (Fig. 2E). Core-only hydrogels degraded by 50% *in vitro* in 6-10 hours, while composites took 3-4 hours to degrade by 50% *in vitro*. Faster degradation was observed in the only weakly cross-linked skirt region compared to the core.

The collagen-based skirt supported growth and proliferation of HCECs, while cells did not appear to populate polypropylene mesh regions (Fig. 2F, G). In collagen composites, the collagen core and skirt were equally cell-populated and were indistinguishable in fluorescence on day 5 post seeding (Fig. 2G).

The impact of material match/mismatch on mechanical behavior of composite hydrogels is shown in Fig.2H,I. When samples were subjected to a tensile force, the polypropylene (PP) mesh-incorporated scaffold ruptured at the interface of collagen and PP mesh, indicating a localized weakness (Fig. 2H). For composites with central core and skirt composed of the same type of collagen, the tensile force was transferred to the central core-only region where the hydrogel was weaker and ultimately ruptured (Fig. 2I).

Microstructural analysis of the core and skirt by electron microscopy revealed that collagen fibers of the skirt formed a more porous structure (Fig. 3A-C) with a degree of localized self-alignment (Fig. 3D,E) whereas the core had a more uniform, but less densely-packed fibril distribution (Fig. 3F). Fiber diameter in the skirt was significantly thinner ($P < 0.001$) than in the core and the native rabbit stroma (Fig. 3G).

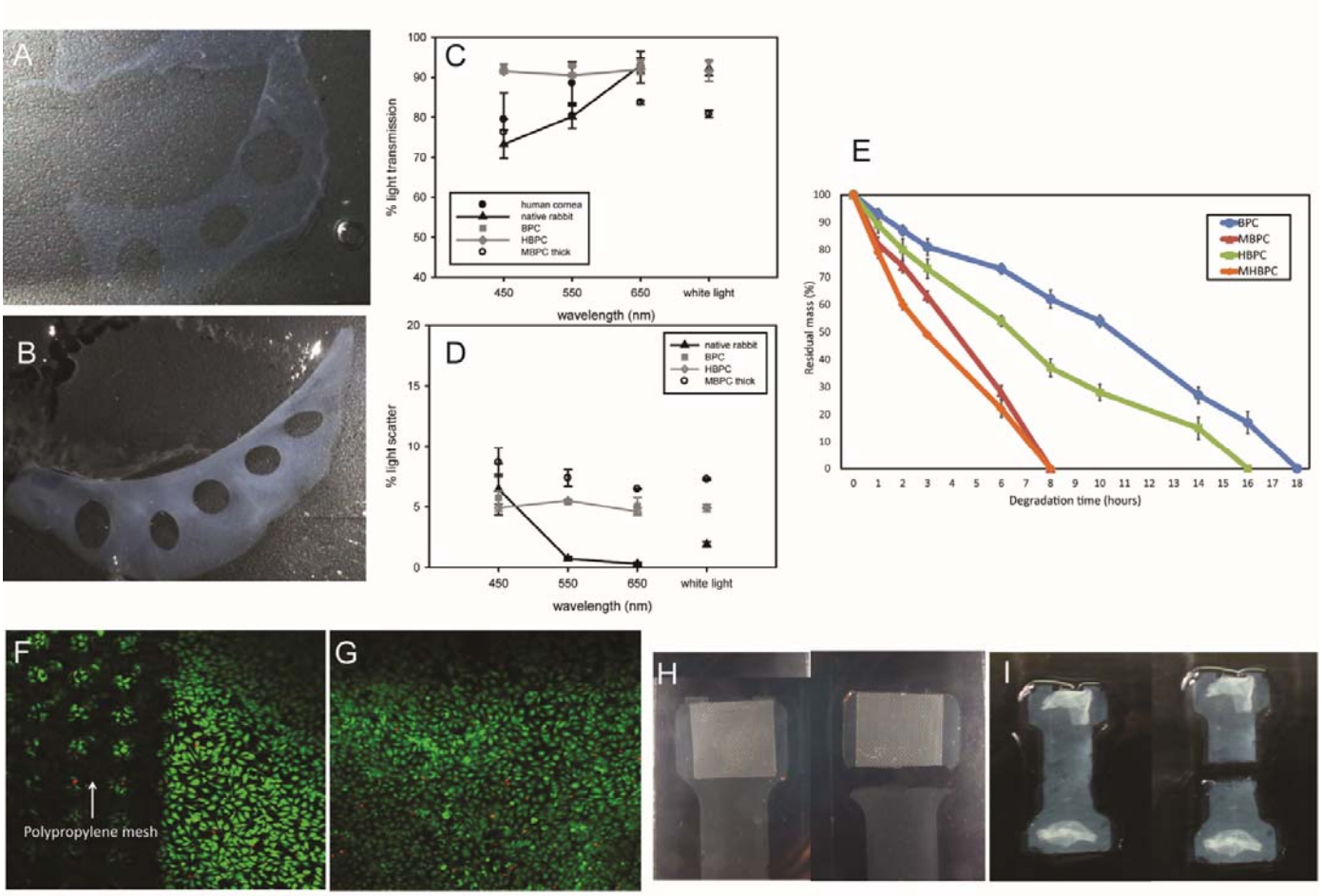

Fig. 2. Ex-vivo characterization of composite hydrogels. Composite BPC implants were fabricated in flat sheets where transparent circles represented the optical core surrounded by a peripheral skirt of reduced transparency. (A) Thin skirt was composed of 1% collagen, 50µm thick. (B) Thick skirt was composed of 2% collagen, 100µm thick. Composites were trephined to include both core and skirt regions in the same circular button intended for implantation. (C) Light transmission and (D) scatter of composite hydrogels. Data for human corneas was the average taken from refs [32-34]. Error bars represent standard deviation (SD) of 3 samples per wavelength**.** (E) Enzymatic degradation indicating composites (MBPC thick, MHBPC) degraded faster than core-only materials (BPC, HPBC) in vitro. (F, G) Confocal microscopy images of human corneal epithelial cells attached to a BPC hydrogel embedded with PP skirt (F) or with collagen skirt MBPC thin (G) on day 5 post seeding. The collagen-based composite supported confluent epithelial cell growth, while grid-patterned PP skirts appeared to prevent their growth (dark areas of PP). (H) Polypropylene (PP) skirt in BPC core, which fractured at the core-skirt interface, despite a uniform/homogeneous distribution of the PP skirt within the core. (I) A collagen skirt resulted in distribution of load within the composite, leading to fracture within the core material. Some non-uniformity in spreading of the collagen skirt was evident, but fracture did not occur at any interface point between core and skirt.

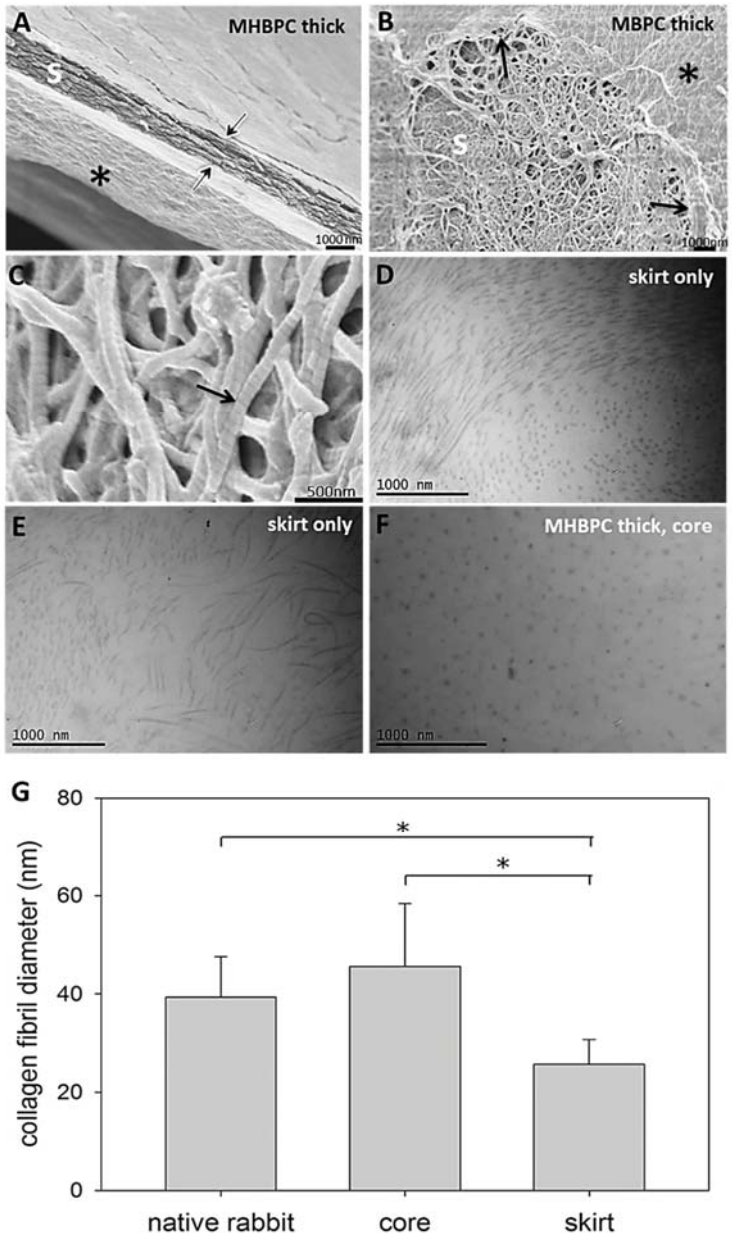

Fig. 3. Electron microscopy of composite biomaterials prior to implantation. Scanning (A-C) and transmission (D-F) electron micrographs. (A) MHBPC thick depicting skirt (s) and core (asterisk) parts. Arrows indicate the cross-section of the skirt exhibiting a porous structure compared to core (asterisk). (B) In MBPC thick, skirt (s) is visible by porous appearance compared to smoother core (asterisk), with black arrows indicating transition from skirt to core. (C) Higher magnification of the skirt from (B) indicating collagen I fibrils with banding seen as parallel lines (arrow). (D, E) Structure of the skirt with loosely-packed collagen fibrils and localized regions of self-alignment. (F) MHBPC thick core with apparent random distribution of loosely-packed collagen fibrils of various diameters. (G) Collagen fibril diameter in native rabbit, central core and peripheral skirt regions, as quantified from transmission images. The skirt had significantly reduced fibril diameter compared to central core and native rabbit stroma ($P<0.001$, one-way ANOVA).

3.2 Operations and postoperative status

All FLISK procedures were performed without intraoperative complications. Native midstromal tissue was extracted and replaced (Fig. 4) with either biomaterial or the same extracted tissue (autograft). Immediately after operation, AS-OCT examination confirmed the intrastromal presence of implants and absence of corneal perforation.

One week postoperatively, severe inflammatory reaction, which included severe haze, purulent excretion and neovascularization, was observed in one cornea implanted with HBPC. Although intensive therapy with steroids and antibiotics was administered, the inflammation did not subside and led to premature sacrifice. Additionally, one rabbit in the MHBPC thick group died while under anesthesia at the 1 month examination. Corneal neovascularization was observed in 2 of 25 corneas 1 month postoperatively (MHBPC thick and autograft). A few corneal neovessels were evident macroscopically (Fig. 5A, B) and microscopically by IVCM (Fig. 5E, F) at 1 month. By three months, the new vessels had subsided without treatment, and were no longer visible in photography (Fig. 5C, D). IVCM revealed signs of regression with vessels of smaller diameter and with phagocytic cells present (Fig. 5G). Histology revealed isolated vessels outside the implanted region surrounded by corneal stroma of normal morphology (Fig. 5H).

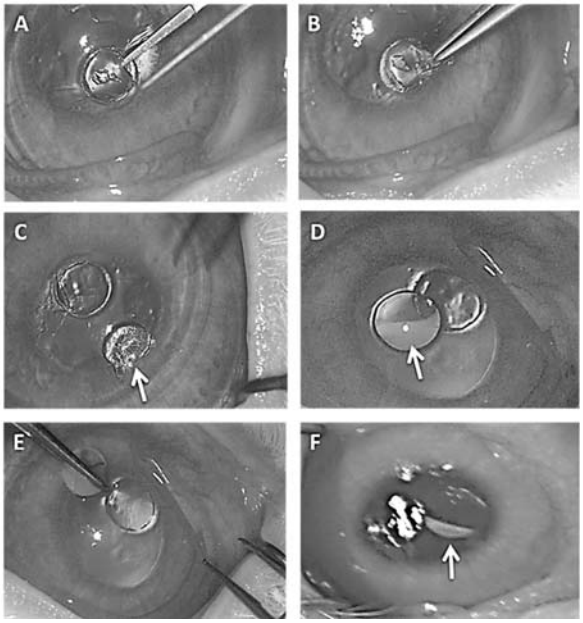

Fig. 4. Manual removal of femtosecond laser cut corneal button and replacement with a composite implant. (A) Insertion of the forceps through the access laser cut to grip the native corneal button cut by the femtosecond laser. (B) Manual removal of the corneal button from the mid-stroma. (C) The corneal button removed and resting on the corneal surface (arrow) with the empty stromal pocket visible. (D) The composite implant with the opaque skirt visible on one side (arrow) is resting on the corneal surface. (E) Manual insertion of the biomaterial into the stromal pocket is achieved by sandwiching the material between surgical forceps. (F) The implant after insertion into the corneal pocket. The opaque peripheral skirt is visible after implantation (arrow).

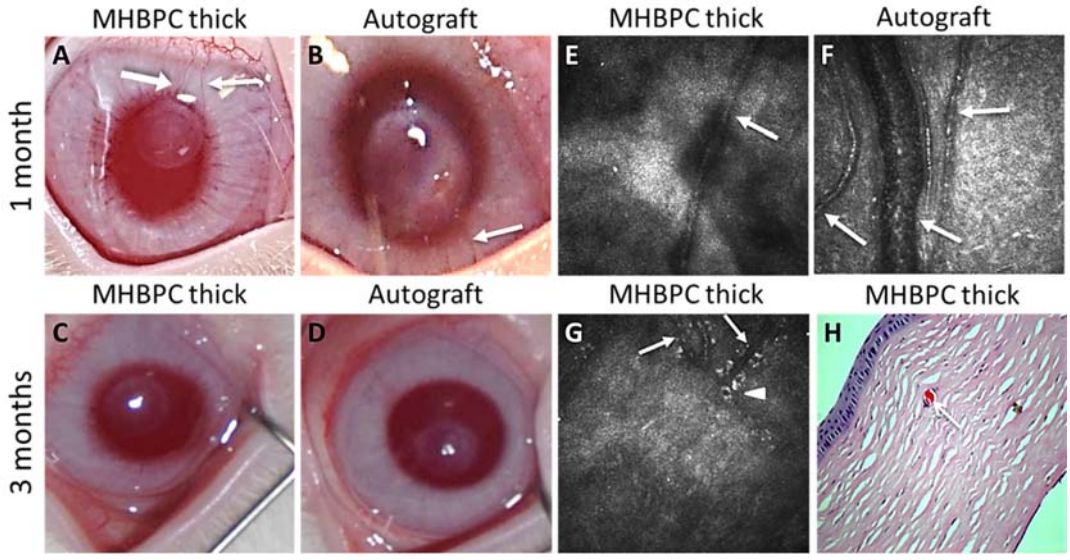

Fig. 5. Postoperative neovascularization in MHBPC thick and autograft corneas. (A,B) Clinical in vivo photographs depicting peripheral neovascularization (white arrows) macroscopically 1 month postoperatively. (C, D) In the same corneas at 3 months, vessels were no longer visible in photographs and transparency improved. (E,F) At 1 month, IVCM images depict perfused vessels (arrows) which at three months (G) became thinner (arrows) with associated

phagocytic cells (arrowhead). (H) H&E staining revealed isolated vessels in otherwise normal-appearing stroma outside the implanted zone.

3.3 Transparency, thickness and degradation of implanted materials

Immediately postoperatively, core and skirt regions were easily visualized in MBPC thick, MBPC thin and MHBPC thick implants (Fig. 6A,D arrows). All corneas (including autografts) had early edema and significantly increased thickness (Fig. 6B) relative to unoperated contralateral corneas ($P= 0.008$), but not relative to autografts (Fig. 6C). As edema subsided corneas reduced in thickness at 1 month ($P=0.025$), with anterior curvature following that of the posterior cornea (Fig. 6D). No further change in corneal thickness was noted after 1 month in any group ($P>0.05$ for all groups). At 3 months, MBPC thin and MHBPC thick groups had significantly thinner corneas than the native rabbit cornea ($P=0.009$ and $P=0.015$, respectively) (Fig. 6B). Autografts and bioengineered implants did not differ significantly in thickness at any postoperative time ($P > 0.05$), with all bioengineered implants retaining about 90% of the autograft thickness (Fig. 6C).

One month postoperatively, the peripheral skirt had degraded and was no longer visible in most composites (Fig. 6A) - only small remnants were observed in two MBPC thick and three MHBPC thick implanted corneas. Core regions in all implants maintained similar transparency to autografts from the first to third postoperative month (Fig. 6A,D). In one cornea from the MBPC thick group and one cornea from the MHBPC thick group, the skirt could still be visualized by AS-OCT at 3 months (Fig. 6E). Histological evaluation confirmed the differential degradation rates of core and skirt parts of the MBPC thick, MBPC thin and MHBPC thick groups. The different parts of the composite were identified by differential staining with the skirt appearing pink (eosinophilic) and core appearing grey/light blue (basophilic) (Fig. 6F). Histology confirmed *in vivo* findings and revealed that remnants of the skirt were absent or very small in all corneas apart from one cornea in the MBPC thick group, which retained a large region of the skirt at 3 months. Postoperative haze in biomaterial-implanted corneas diminished over time and was similar to autografts at 3 months (Fig. 6A,D).

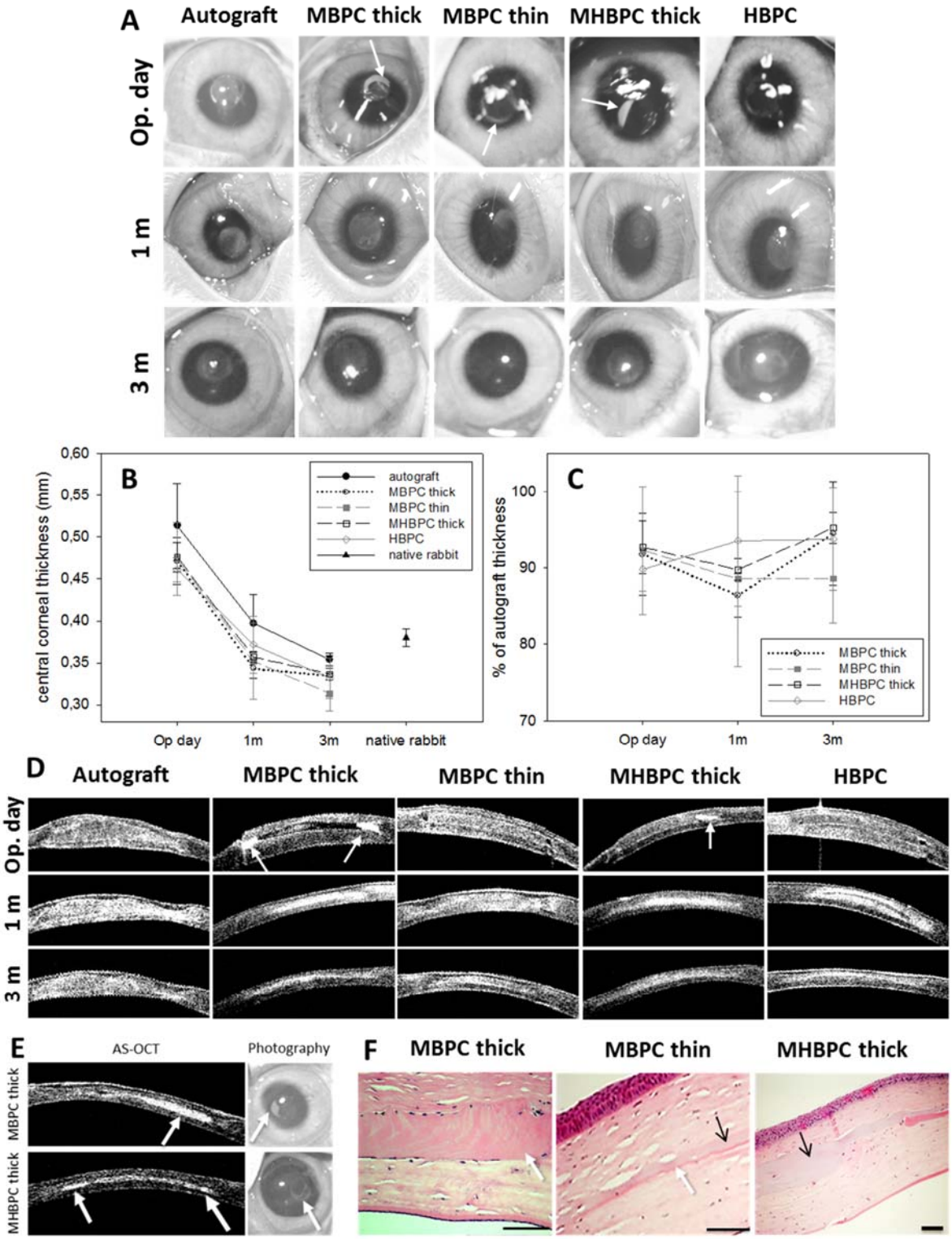

Fig. 6. Transparency, thickness and degradation of composite implants. (A) serial clinical in vivo photographs of the same cornea in each experimental group. The skirt was easily visualised postoperatively in the periphery of the implants (arrows) in MBPC thick, MBPC thin and MHBPC thick groups (first row). The mesh part had degraded restoring transparency after

1 month (second row) or after 3 months (third row). Postoperative haze in biomaterial groups resembled haze in the autograft group and gradually diminished with time. (B) In vivo central corneal thickness as mean and standard deviation (error bars) of measurements from five corneas from each group and 3 measurements per cornea, with the exception of MHBPC thick and HBPC groups which had four corneas each. (C) Thickness of implanted corneas relative to autografts. (D) Longitudinal AS-OCT images of the same corneas postoperatively. Initial edema subsided by 1 month while the skirt region visible directly after operation by increased reflectivity (arrows), was no longer visible after 1 and 3 months in all but two cases. Light scatter subsided at 3 months and was consistent with a minimal haze observed clinically. (E) In two rabbits at 3 months, the skirt (arrows) was visible in photography and AS-OCT. (F) H&E sections of the two rabbit corneas depicted in (E) with partial skirt present at 3 months as well as one cornea of MBPC thin group where a very thin remnant of the skirt was visible in histologically but not clinically (black and white arrows depict core and skirt, respectively). Scale bars: 100 μm.

3.4 Wound healing

Immunohistochemical analysis revealed variable expression of type III (scar-type) collagen (Fig. 7A-C). Most corneas either minimally expressed or were negative for collagen III (Fig. 7A, C), while a minority exhibited intense staining for collagen III (Fig. 7B). This trend was not confined to a specific group but appeared to vary with the individual response to injury following operation. α-SMA+ cells tended to be accumulate at implant borders in certain corneas exhibiting collagen III staining, implicating α-SMA+ stromal myofibroblasts as the source of the type III collagen (Fig. 7D-F). Absence of scar tissue in some cases and the close apposition of cells to the implants was also confirmed by transmission electron microscopy (Fig. 7G,H). After 3 months in vivo, the core exhibited a homogenous, amorphous structure with no visible collagen fibrils (Fig. 7G) while the skirt maintained some ultrafine fibrillary organization (Fig. 7H).

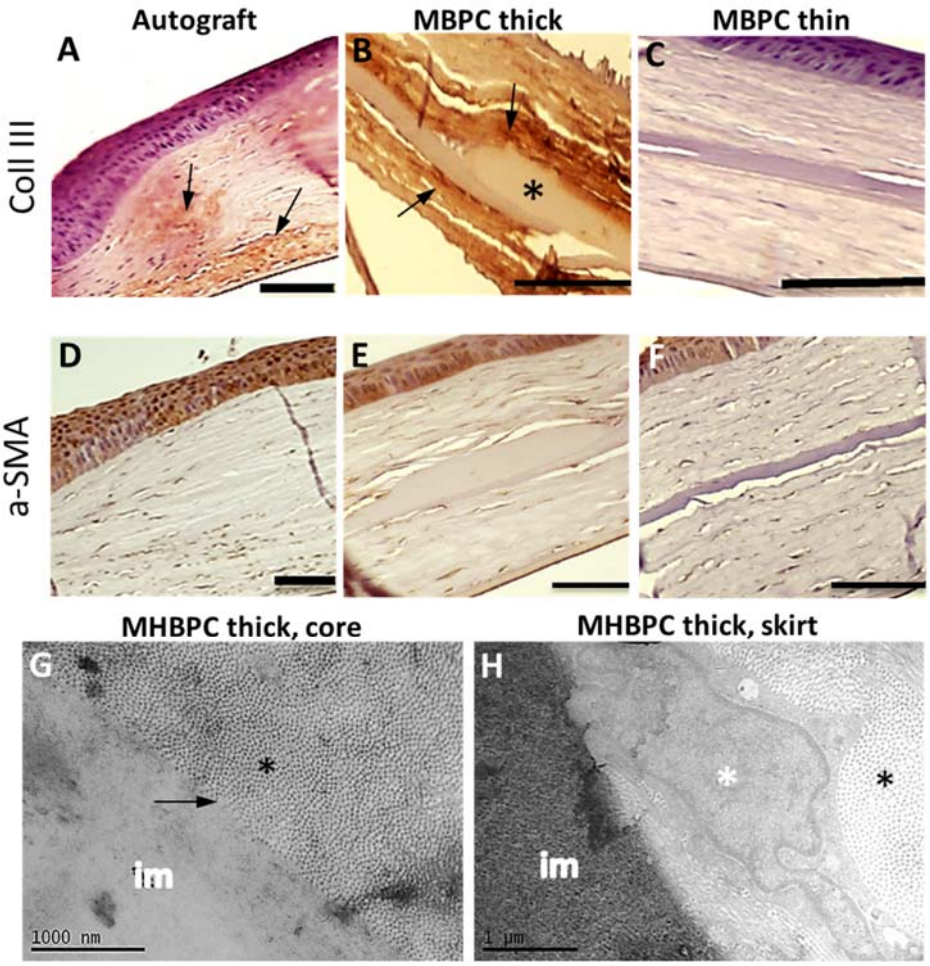

Fig. 7. Immunohistochemical and TEM analysis of healing in implanted corneas. (A) Representative autograft with minimal to moderate collagen III staining, localized at interfaces (arrows). (B) Rare intense positive staining for collagen III at stromal-implant interfaces (arrows) in the single implant retaining a thick skirt (asterisk) at 3 months. (C) Absence of collagen III staining in MBPC thin implanted cornea. (D-F) Stroma of the same corneas depicted in A-C was populated with α-SMA^{+} myofibroblasts to variable extent. (G) MHBPC group depicting the core area (im) without apparent collagen fibril structure and adjacent native stroma (black asterisk) with collagen fibers of remarkably uniform diameter and interfibrillar space. No disorganized scar tissue was present at the implant-host interface (arrow). (Note: the intense black formations are artifacts). (H) A cell (white asterisk), either fibroblast or macrophage, was observed at the host (black asterisk) - skirt (im) interface, in direct contact with the implant. No scar tissue was observed at the interface. The skirt part of the implant (im in H) had an ultrafine structure that was disorganized relative to native stroma (black asterisks in G and H). Scale bars (A-F): 100 µm.

3.5 Nerve status

IVCM examination revealed coverage of all implanted corneas by epithelium postoperatively.

The corneal epithelium derives innervation from the subbasal nerve plexus, which was

visualized by IVCM. No significant difference in subbasal nerve density was found between native rabbit cornea, biomaterial or autografts at three months (Fig. 8A), and nerve morphology appeared normal with thin nerve fibers running roughly parallel (Fig. 8B). A stromal nerve was observed regenerating into the biomaterial at the host-to-implant interface in one rabbit of the MHBPC thick group at 3 months (Fig. 8C). The superficial access cut made by the femtosecond laser was repopulated by regenerated subbasal nerves by one month after operation (Fig. 8D).

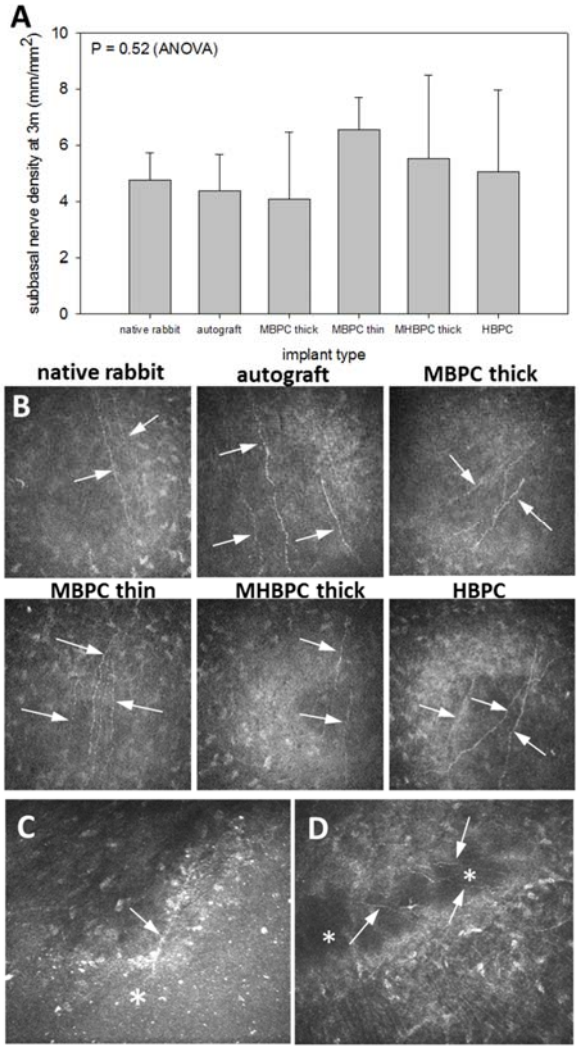

Fig. 8. Nerve regeneration and nerve presence in implanted corneas. (A) A normal density of nerves in the subbasal plexus layer was maintained in all implanted groups at three months, indicating minimal impact of the implantation procedure and implanted biomaterials on the corneal epithelial status. (B) Subbasal nerves (arrows) were present in all groups with a normal morphology and density distribution. (C) A regenerating stromal nerve (arrow) entering the implanted biomaterial (asterisk) in one cornea of the MHBPC thick group three months

postoperatively. (D) Subbasal nerves (arrows) regenerating across the laser cut region (asterisks) in MBPC group one month postoperatively.

3.6 Stromal cell migration following implantation

Corneal examination at the cellular level was conducted *in vivo* by IVCM, and *ex vivo* by H&E and immunohistochemical staining. IVCM of core-skirt peripheral interfaces revealed round or oval-shaped reflective cells with dark nucleus at one and three months, in close proximity to visible skirt remnants (Fig. 9A). As previously described [35], this cell morphology corresponds to mature macrophages, which were also found in autografts. The central implanted region (Fig. 9B) in autografts was populated by stromal keratocytes while in biomaterials, sparse keratocyte-like and macrophage-like cells were observed within the implant material. Histochemical staining confirmed that initially acellular implants were populated with host cells at three months (Fig. 9C). Cells were found in both core and in remnants of the skirt, and consisted of α-SMA+ myofibroblasts originating from activated keratocytes and/or CD45+ bone marrow-derived cells (Fig. 9D) such as macrophages [36,37]. Although inflammatory cells were observed *in vivo* and *ex vivo*, no signs of inflammation were noted upon clinical examination of implanted eyes at three months.

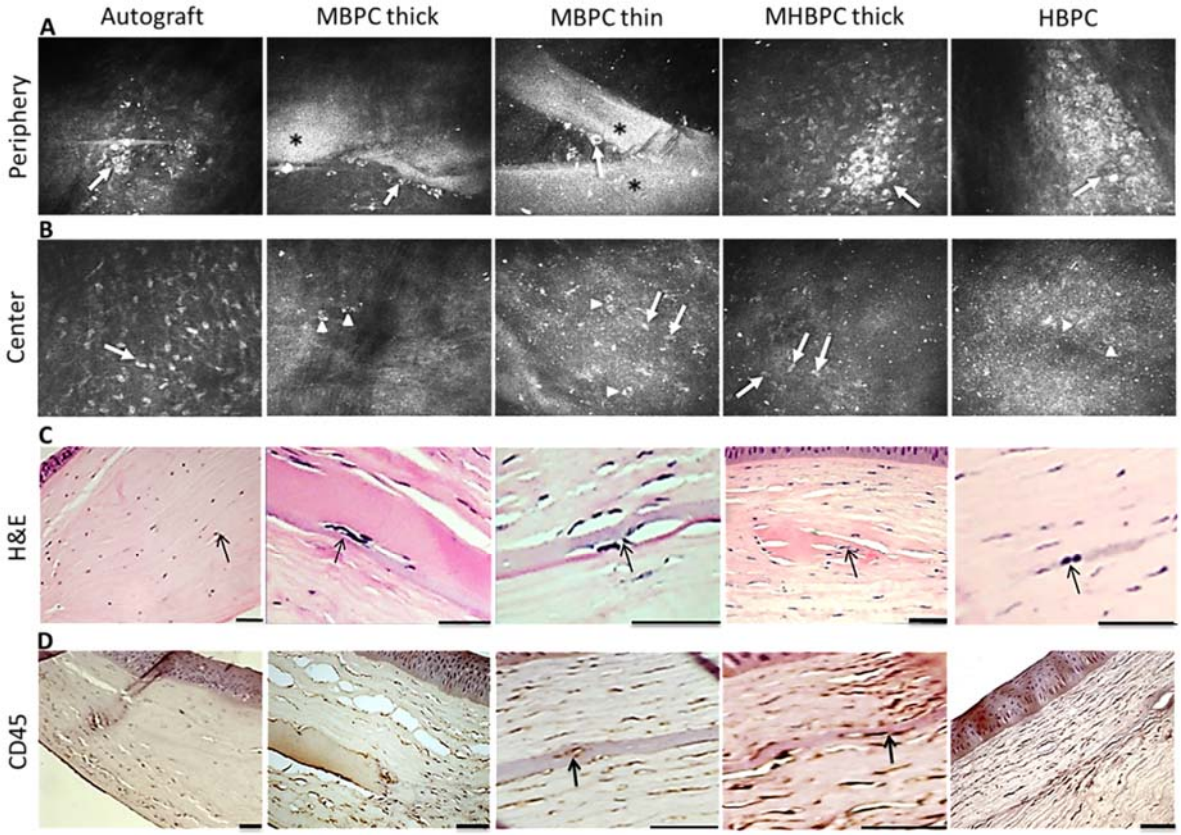

Fig. 9. Migration of host cells into core and skirt regions. Row (A) IVCM of peripheral implant interface; (B) IVCM of central implant; (C) H&E staining; (D) Immunostaining for CD45. (A) Mature macrophages (arrows) were present in all groups including autografts, at interfaces, around implant borders and skirt regions. Highly light-scattering areas in MBPC thick and MBPC thin corresponded to remnants of the peripheral skirt (black asterisks). (B) Host cells within central implants in all groups (arrowheads indicate macrophages and arrows indicate keratocyte-like cells). (C) H&E sections confirmed the presence of host cells within implants and partially degraded skirt regions. Black arrows indicate cells within the implants. (D) CD45+ cells were found in both autograft and biomaterial groups. The black arrows indicate CD45+ cells within implants. Scale bars: 50 µm

4 Discussion

Here we report the first core-and-skirt composite type I collagen hydrogels for corneal applications. Composites were biocompatible and integrated with host cells, nerves, and collagen of the native stroma. The non-crosslinked skirt region degraded faster *in vitro* and *in vivo* than the core. As the partially opaque skirt degraded, hydrogels regained transparency, with macrophages accumulating at skirt and core interfaces, likely accumulating to remove the breakdown products. Breakdown and skirt removal occurred without signs of clinical

inflammation. Tunable skirt thickness enabled control of degradation rate (the thicker skirt with higher collagen content degraded more slowly), while the tunable skirt transparency enabled *in vivo* tracking of degradation by microscopy and clinical photography. Moderately opaque peripheral skirts were used for investigational purposes; however, other designs are feasible, such as a fully transparent skirt present throughout the hydrogel.

Composite core-and-skirt designs have been used to improve integration of biologically inert synthetic prostheses with the surrounding host tissue [4, 7-12]. The composite developed here is fundamentally different from an inert prosthetic material, because it is biodegradable and designed to interact with surrounding host tissue and stimulate endogenous corneal regeneration, with eventual replacement by natural stroma through population by host keratocytes and fibroblasts which remodel the extracellular matrix [14]. The composite hydrogels in this study do not require a peripheral skirt for proper integration into the host stroma, but the skirt is designed to facilitate degradation for therapeutic cell and substance release. Biodegradation and population of the skirt by host cells indicates the skirt can support migrating cells to potentially deliver therapeutic agents such as stem cells (shown to be compatible with the BPC materials [14]) or drugs to the cornea. Agents such as cells or growth factors could be incorporated into the skirt region for delivery of specific therapy while the central core functions as a longer-term stromal scaffold for maintaining the structure and optical transparency of the cornea. The central core is expected to degrade slowly as host stromal cells repopulate and replace it with host collagen [14], with complete long-term replacement of the core by host stroma expected to take several years.

Another important difference from prior composite keratoprosthesis designs is that biologically inert materials require surface modifications or coating with collagen or other growth factors to support cell adhesion, and special steps to maintain permeability for nutrient diffusion for cell survival [7, 9-12]. Construction of inert prostheses with regenerative capacity therefore includes many technically demanding steps [9, 11, 12]. Alternatively, composites presented here are composed of a safe and well-characterized medical-grade porcine collagen not requiring surface modification.

In vivo tracking of skirt degradation was achieved without the use of potentially toxic markers or fluorescent agents, with degradation observable by direct clinical observation and

photography. Near complete degradation occurred during the first postoperative month in most composites, although some variability was present with remnants visible at 3 months in a few cases. This finding demonstrates that the skirt can be tuned to achieve either fast degradation or a prolonged presence in the corneal stroma.

Tunability of skirt transparency was enabled by changing the initial concentration of skirt collagen from 1 to 2% and skirt thickness from 50µm to 100µm. Increasing collagen concentration in the skirt (followed by mechanical compression) reduces the penetration of core collagen/cross-linker solution into the skirt, resulting in a more abrupt core-skirt interface, greater refractive index mismatch, and reduced transparency. By contrast, core transparency can be maintained over a wide range of collagen concentration [14, 15, 28], and it is believed that collagen fibril structure and diameter are more important for maintaining transparency in the homogeneous core. Core fibril diameter in this study, prior to implantation, was comparable to the native rabbit stromal collagen fibril diameter.

The BPC core consisted of a single chemically-crosslinked polymer network, while HBPC hybrid core was composed of at least two chemically-crosslinked polymer networks. The skirt acts as an additional supporting collagen network embedded into the main collagen scaffold to provide load-distribution when subjected to external forces such as those encountered during implantation surgery. In the case of MHBPC, the skirt and one of the polymer networks are based on biopolymers, e.g. collagen, while the second network is a synthetic polymer. HBPC/MHBPC results demonstrate that the composite design supports various types of core material and crosslinking architecture, giving flexibility in the design of core and skirt properties for specific therapeutic applications.

In order to study the regeneration within the corneal stroma and minimize surgically-stimulated wound healing induced after epithelial trauma [36, 37], a recently developed non-disruptive surgical technique (FLISK) [14] was used for intrastromal implantation. The procedure was carried out successfully with only one rejection episode observed one week postoperatively due to severe inflammation. Type III collagen, characteristic of scar tissue, was found in similar amounts in autograft and biomaterial groups and was localized at the host-implant interface. Clinical observation of a slight haze was consistent with minimal collagen III staining and scar formation, indicating that transparency can be maintained with minimal

collagen III production. Thicker implants, replacing a greater proportion of the native stroma, and an implantation technique such as deep anterior lamellar keratoplasty (DALK), can be expected to further reduce the haze at host-implant interfaces.

Neovascularization was noted in two rabbits one month after implantation, but by 3 months, vessels regressed. Vascularization of an autografted cornea indicated that neovascularization was stimulated by surgery and not the implant material. Nevertheless, identification of inflammatory cells near and within implants confirmed that cell migration was supported by both core and skirt. Inflammatory cell presence in autograft-implanted corneas suggests a mild, subclinical inflammatory response to the surgery in some cases. Femtosecond lasers are used in corneal refractive surgery due to improved reproducibility, safety and precision [38] but the surgery can contribute to an inflammatory response compared to the traditional mechanical methods [39]. Reasons are an increased number of stromal cells that undergo necrosis as direct result of the stromal laser ablation [40]. This inflammatory response, however, is mild with little or no effect on visual acuity [39] and can be influenced by adjusting energy levels [39-41]. Although in FLISK epithelial damage is minimized by creating a small access cut, injured epithelial cells and keratocytes that underwent apoptosis after the ablation could stimulate inflammatory cell migration. In addition, breakdown of the collagen skirt is expected to have stimulated macrophage recruitment. These signs of inflammation, however, could only be detected at the microscopic level and were invisible clinically.

Neither FLISK nor the biomaterials disturbed the anatomical structures of the cornea outside the implanted zone. In particular, corneal nerves within the subbasal nerve plexus had normal density and morphology in all groups after 3 months. Nerve regrowth was observed in the access cut as early as one month postoperatively, indicating quick nerve recovery following this minimally disruptive technique. As the access cut covered only 70° of the circumference of the implant, subbasal nerves in the majority of the epithelium were spared by the FLISK procedure. The subbasal nerve plexus is of vital importance to the health of the cornea, as these nerves gives rise to sensations of touch, pain and temperature, the protective blink reflex, sufficient production of tears, and wound healing. Although most types of laser and corneal transplant surgery result in corneal de-nervation leading to a neurotrophic deficit [42], the FLISK procedure appears to preserve the epithelium and its nerve population. Apart from preservation of the epithelial nerves, new nerve ingrowth into the stromal core part of the

implant was noticed 3 months after implantation in one cornea, indicating that the BPC material has the potential to support nerve in-growth. In earlier versions of crosslinked hydrogels implanted by deep anterior lamellar keratoplasty, nerves within the stroma were observed starting at two months [43]. A longer follow-up time may allow the regeneration of more stromal nerves into the composite implants as well.

Maintenance of shape and corneal transparency are two basic requirements of bioengineered materials for vision-restoring therapeutic applications in the cornea. Although the MBPC thin and MHBPC corneas were thinner than native rabbit corneas after 3 months *in vivo*, no significant thickness difference was noted between the composite implants and the autografted corneas. All groups maintained thickness relative to autografts within a 10-15% margin, which can be attributed to breakdown of the mesh and/or slight dehydration of implants. These changes can be counteracted in future studies by increasing thickness of the core material. Larger groups are required in future studies, to optimize core and skirt materials and thicknesses to achieve a desired speed of degradation while maintaining a desired total corneal thickness for a given application. Notably, the suitability of compressed collagen gels (similar to the skirt in this study) to act as scaffolds onto which limbal stem cells are cultured for the construction of an artificial corneal epithelium has already been tested [44,45]. Corneal epithelial cells are shown to adhere, proliferate, differentiate and stratify on compressed collagen significantly better than on conventional uncompressed collagen [44]. This was attributed to the structural similarity between the compressed collagen gel and the normal corneal stroma, as seen in SEM and TEM [44]. Moreover, compressed collagen gels were easy to handle and had sufficient mechanical strength for surgical use [45].

Microstructural analysis of composites prior to implantation indicated sparse collagen fibers within the core. After 3 months *in vivo*, the core exhibited a homogenous, non-lamellar ultrastructure with no clear collagen fibrils visible similar to an earlier study with core-only BPC [14]. By contrast, collagen fibers of the skirt were more homogeneous in diameter, partially aligned and more densely packed. After three months, despite absence of clear collagen fibril structure, the skirt exhibited an ultrafine structure that more closely mimicked the native corneal stroma, in accordance with earlier studies detailing the microstructure of compressed collagen [16, 44]. While the specific mechanisms of collagen transformation after

implantation require further investigation, the high degree of corneal transparency observed post implantation and during skirt degradation is promising.

Finally, besides cell delivery, composite collagen hydrogels could restore optical clarity in scar-forming corneal diseases while potentially delivering drugs intra-stromally. Because the corneal epithelium along with the tear fluid drainage poses a significant barrier to topical drug delivery into the cornea, targeted intra-stromal drug injections have been recently utilized [46,47]. However, these injections pose the risk of corneal perforation, are invasive, and cannot facilitate controlled, slow release drug delivery. For such applications, composite hydrogels could act as biodegradable implants containing encapsulated drugs for spatially and temporally-controlled release in the corneal stroma. Such an application requires further investigation.

5 Conclusion

In conclusion, unloaded, cell-free composite collagen-based hydrogels are biocompatible scaffolds that additionally support differential, spatially-controlled degradation. Degradation rate can be tuned by thickness, degree of crosslinking, and collagen content of an embedded skirt, with the *in vitro* collagenase assay providing an indication of relative degradation performance *in vivo*. Control of skirt transparency by collagen content and thickness enabled non-invasive, in vivo tracking of skirt degradation in the eye by monitoring restoration of transparency in the skirt region. Compatibility with host cells and nerves, and maintenance of corneal shape, transparency and thickness by composites was similar to autograft implanted tissue. Composite implants represent a feasible platform for future cell and drug delivery into the cornea, to address cases of corneal blindness which no single homogeneous engineered biomaterial can treat today.

Acknowledgements

The authors wish to sincerely thank Dr. Amy Gelmi for assistance with SEM imaging, Dr. Adrian Elizondo for HCEC work, Catharina Traneus-Röckert for immunohistochemical staining, Gertrud Strid for H&E staining, and Abeni Wickham for assistance with early versions of the collagen mesh preparation. The authors wish to additionally acknowledge the kind contribution of Abbott Medical Optics (Swedish and UK affiliates) for technical assistance in the development of the FLISK procedure, which is presently an off-label use of the IntraLase iFs 150 kHz femtosecond laser. The authors have also received an unrestricted educational grant from Abbott Medical Optics Inc, Solna, Sweden, to perform the femtosecond laser procedures. One author of this publication (Mehrdad Rafat) holds stock in the company LinkoCare Life Sciences AB which is developing products related to the research being reported and holds relevant patents. Mehrdad also serves on the Board of Directors of the company. The terms of his arrangements have been reviewed and approved by Linköping University in accordance with its policy on objectivity in research. For the remaining authors, no competing financial interests exist.

References

[1] Robaei D, Watson S. Corneal blindness: a global problem. Clin Experiment Ophthalmol 2014;42(3):213-4.

[2] Wang HY, Wei RH, Zhao SZ. Evaluation of corneal cell growth on tissue engineering materials as artificial cornea scaffolds. Int J Ophthalmol. 2013;6(6):873-8. doi: 10.3980/j.issn.2222-3959.2013.06.23.

[3] Wang L, Ma R, Du G, Guo H, Huang Y. Biocompatibility of helicoidal multilamellar arginine-glycine-aspartic functionalized silk biomaterials in a rabbit corneal model. J Biomed Mater Res B Appl Biomater. 2014 May 13. doi: 10.1002/jbm.b.33192.

[4] Jiang H, Zuo Y, Zhang L, Li J, Zhang A, Li Y, Yang X. Property- based design: optimization and characterization of polyvinyl alcohol (PVA) hydrogel and PVA-matrix composite for artificial cornea. J Mater Sci Mater Med. 2014;25(3):941-52. doi: 10.1007/s10856-013-5121-0.

[5] Alaminos M, Sánchez-Quevedo MDC, Munoz-Ávila JI, Serrano D, Medialdea S, Carreras I, Campos Antonio. Construction of a complete rabbit cornea using a fibrin-agarose scaffold. Invest Ophthalmol Vis Sci. 2006;47:3311–3317. doi:10.1167/iovs.05-1647

[6] Zhang Q, Su K, Chan-Park MB, Wu H, Wang D, Xu R. Development of high refractive ZnS/PVP/PDMAA hydrogel nanocomposites for artificial cornea implants. Acta Biomater. 2014;10(3):1167-76. doi: 10.1016/j.actbio.2013.12.017.

[7] Myung D, Duhamel PE, Cochran J, Noolandi J, Ta C, Franl C. Development of hydrogel-based keratoprosthesis: a materials perspective. Biotechnol Prog. 2008;24(3):735-741. Doi:10.1021/bp070476n.

[8] Fenglan X, Yubao L, Xiaoming Y, Hongbing L, Li Z. Preparation and in vivo investigation of artificial cornea made of nano-hydroxyapatite/poly (vinyl alcohol) hydrogel composite. J Mater Sci Mater Med. 2007;18(4):635-40.

[9] Myung D, Koh W, Bakri A, Zhang F, Marshall A, Ko J, Noolandi J, Carrasco M, Cochran JR, Frank CW, Ta CN. Design and fabrication of an artificial cornea based on a photolithographically patterned hydrogel construct. Biomed Microdevices. 2007;9(6):911-22.

[10] Bakhshandeh H, Soleimani M, Hosseini SS, Hashemi H, Shabani I, Shafiee A, Nejad AH, Erfan M, Dinarvand R, Atyabi F. Poly (ε-caprolactone) nanofibrous ring surrounding a polyvinyl alcohol hydrogel for the development of a biocompatible two-part artificial cornea. Int J Nanomedicine. 2011;6:1509-15. doi: 10.2147/IJN.S19011.

[11] Zellander A, Gemeinhart R, Djalilian A, Makhsous M, Sun S, Cho M. Designing a gas foamed scaffold for keratoprosthesis. Mater Sci Eng C Mater Biol Appl. 2013;33(6):3396-403. doi: 10.1016/j.msec.2013.04.025.

[12] Zellander A, Wardlow M, Djalilian A, Zhao C, Abiade J, Cho M. Engineering copolymeric artificial cornea with salt porogen. J Biomed Mater Res A. 2014;102(6):1799-808. doi: 10.1002/jbm.a.34852.

[13] Fagerholm P, Lagali NS, Ong JA, Merrett K, Jackson WB, Polarek JW, Suuronen EJ, Liu Y, Brunette I, Griffith M. Stable corneal regeneration four years after implantation of a cell-free recombinant human collagen scaffold. Biomaterials. 2014;35(8):2420-7. doi: 10.1016/j.biomaterials.2013.11.079.

[14] Koulikovska M, Rafat M, Petrovski G, Vereb Z, Akhtar S, Fagerholm P, Lagali N. Enhanced Regeneration of Corneal Tissue via a Bioengineered Collagen Construct implanted by a Non-disruptive Surgical Technique. Tissue Eng Part A. 2015;21:1116-30.

[15] Liu Y, Gan L, Carlsson DJ, Fagerholm P, Lagali N, Watsky MA, Munger R, Hodge WG, Priest D, Griffith M. A simple, cross-linked collagen tissue substitute for corneal implantation. Invest Ophthalmol Vis Sci. 2006;47(5):1869-75.

[16] Xiao X, Pan S, Liu X, Zhu Z, Connon CJ, Wu J, Mi S. In vivo study of the biocompatibility of a novel compressed collagen hydrogel scaffold for artificial corneas. J Biomed Mater Res A. 2014;102(6):1782-7. doi: 10.1002/jbm.a.34848.

[17] van Essen TH, Lin CC, Hussain AK, Maas S, Lai HJ, Linnartz H, van den Berg TJ, Salvatori DC, Luyten GP, Jager MJ. A fish scale-derived collagen matrix as artificial cornea in rats: properties and potential. Invest Ophthalmol Vis Sci. 2013;54(5):3224-33. doi:10.1167/iovs.13-11799.

[18] Yuan F, Wang L, Lin CC, Chou CH, Li L. A cornea substitute derived from fish scale: 6-month follow up on rabbit model. J Ophthalmol. 2014;2014:914542. doi: 10.1155/2014/914542.

[19] Griffith M, Polisetti N, Kuffova L, Gallar J, Forrester J, Vemuganti GK, Fuchsluger TA. Regenerative approaches as alternatives to donor allografting for restoration of corneal function. Ocul Surf. 2012;10(3):170-83. doi: 10.1016/j.jtos.2012.04.004.

[20] Sejpal K, Bakhtiari P, Deng SX. Presentation, Diagnosis and Management of Limbal Stem Cell Deficiency. Middle East Afr J Ophthalmol. 2013;20(1):5-10. doi: 10.4103/0974-9233.106381.

[21] Singh P1, Tyagi M, Kumar Y, Gupta KK, Sharma PD. Ocular chemical injuries and their management. Oman J Ophthalmol. 2013;6(2):83-6. doi: 10.4103/0974-620X.116624.

[22] Clements JL, Dana Reza. Inflammatory corneal neovascularization: etiopathogenesis. Semin Ophthalmol. 2011;26(4-5):235-45. doi: 10.3109/08820538.2011.588652.

[23] Burman S, Sangwan V. Cultivated limbal stem cell transplantation for ocular surface reconstruction. Clinical Ophthalmology 2008;2(3):489-502.

[24] Feng Y, Borrelli M, Reichl S, Schrader S, Geerling S. Review of alternative carrier materials for ocular surface reconstruction. Curr Eye Res. 2014;39(6):541-52. doi: 10.3109/02713683.2013.853803.

[25] Ziaei M1, Sharif-Paghaleh E, Manzouri B. Pharmacotherapy of corneal transplantation. Expert Opin Pharmacother. 2012;13(6):829-40. doi: 10.1517/14656566.2012.673588.

[26] Ghate D, Edelhauser H.F. Barriers to glaucoma drug delivery. J. Glaucoma 2008;17(2):147-156.

[27] Kim YC, Chiang B, Wu Xianggen, Prausnitz MR. Ocular delivery of macromolecules. J Control Release. 2014;190:172-81. doi: 10.1016/j.jconrel.2014.06.043.

[28] Rafat, M., Li, F., Fagerholm, P., Lagali, N.S., Watsky, M.A., Munger, R., et al. PEG-stabilized carbodiimide cross linked collagen-chitosan hydrogels for corneal tissue engineering. Biomaterials 2008;29**:**3960.

[29] Priest D, Munger R. A new instrument for the monitoring of the optical properties of corneas. Invest Ophthalmol Vis Sci 39(suppl), s352, 1998.

[30] Lagali N, Griffith M, Fagerholm P. In vivo confocal microscopy of the cornea to assess tissue regenerative response after biomaterial implantation in humans. Methods Mol Biol. 2013;1014:211-23. doi: 10.1007/978-1-62703-432-6_15.

[31] Lagali N, Peebo BB, Germundsson J, Edén U, Danyali R, Rinaldo M, Fagerholm P. Laser-scanning in vivo confocal microscopy of the cornea: imaging and analysis methods for preclinical and clinical applications. Intech 2013;4:51-80.

[32] Meek, K.M., Leonard, D.W., Connon, C.J., Dennis, S., and Khan, S. Transparency, swelling and scarring in the corneal stroma. Eye **17**, 927, 2003.

[33] Beems, E.M., and van Best, J.A. Light transmission of the cornea in whole human eyes. Exp Eye Res **50**, 393, 1990.

[34] Freegard, T.J. The physical basis of transparency of the normal cornea. Eye **11**, 465, 1997.

[35] Peebo BB, Fagerholm P, Traneus-Röckert C, Lagali N. Cellular level characterization of capillary regression in inflammatory angiogenesis using an in vivo corneal model. Angiogenesis. 2011;14(3):393-405. doi: 10.1007/s10456-011-9223-3.

[36] Wilson SE. Corneal myofibroblast and pathobiology: Generation, persistence and transparency. Exp Eye Res. 2014;99(1):78-88.doi:10.1016/j.exer.2012.03.018.

[37] Torricelli AA, Wilson SE. Cellular and extracellular matrix modulation of corneal stromal opacity. Exp Eye Res. 2014. pii: S0014-4835(14)00263-2. doi: 10.1016/j.exer.2014.09.013.

[38] Kymionis GD, Kankariya VP, Plaka AD, Reinstein DZ. Femtosecond laser technology in corneal refractive surgery: a review. J Refract Surg. 2012;28(12):912-20. doi: 10.3928/1081597X-20121116-01.

[39] de Paula FH, MD, Khairallah CG, Niziol LM, Musch DC, Shtein RM. Diffuse lamellar keratitis after laser in situ keratomileusis with femtosecond laser flap creation. J Cataract Refract Surg. 2012;38(6):1014–1019. doi:10.1016/j.jcrs.2011.12.030.

[40] Netto MV, Mohan RR, Medeiros FW, Dupps WJ Jr, Sinha S, Krueger RR, Stapleton WM, Rayborn M, Suto C, Wilson SE. Femtosecond laser and microkeratome corneal flaps: comparison of stromal wound healing and inflammation. J Refract Surg 2007;23:667–676.

[41] de Medeiros FW, Kaur H, Agrawal V, Chaurasia SS, Hammel J, Dupps WJ, Wilson SE. Effect of Femtosecond Laser Energy Level on Corneal Stromal Cell Death and Inflammation. J Refract Surg. 2009;25(10):869–874. doi:10.3928/1081597X-20090917-08.

[42] Shaheen BS, Bakir M, Jain S. Corneal nerves in health and disease. Surv Ophthalmol. 2014;59(3):263-85. doi: 10.1016/j.survophthal.2013.09.002.

[43] Lagali NS, Griffith M, Shinozaki N, Fagerholm P, Munger R. Innervation of Tissue-Engineered Corneal Implants in s Porcine Model: A 1-Year In Vivo Confocal Microscopy Study. Invest Ophthalmol Vis Sci. 2007;48:3537-3544. Doi:10.1167/iovs.06-1483.

[44] Shengli M, Chen B, Wright B, Connon CJ. Plastic compression of a collagen gel forms a much improved scaffold for ocular surface tissue engineering over conventional collagen gels. J Biomed Mater Res A. 2010;95(2):447-53. doi: 10.1002/jbm.a.32861.

[45] Levis HJ, Brown RA, Daniels JT. Plastic compressed collagen as a biomimetic substrate for human limbal epithelial cell culture. Biomaterials 2010;31(30):7726-37. doi: 10.1016/j.biomaterials.2010.07.012.

[46] Pallikaris IG, Kymionis GD, Plaka AD, Binder PS, Kontadakis GA, Tsoulnaras KI. Femtosecond Laser-Assisted Intra-Corneal Drug Delivery. Semin Ophthalmol. 2014 Feb 7.

[47] Hashemian MN, Zare MA, Rahimi F, Mohammadpour M. Deep intrastromal bevacizumab injection for management of corneal stromal vascularization after deep anterior lamellar keratoplasty, a novel technique. Cornea 2011;30:215–218.